

See discussions, stats, and author profiles for this publication at: <https://www.researchgate.net/publication/6707375>

Current Rectification with Poly- l -Lysine-Coated Quartz Nanopipettes

ARTICLE in NANO LETTERS · DECEMBER 2006

Impact Factor: 13.59 · DOI: 10.1021/nl061681k · Source: PubMed

CITATIONS

101

READS

37

6 AUTHORS, INCLUDING:



Senkei Umehara

Japan Science and Technology Agency (JST)

15 PUBLICATIONS 277 CITATIONS

[SEE PROFILE](#)



Nader Pourmand

University of California, Santa Cruz

127 PUBLICATIONS 3,329 CITATIONS

[SEE PROFILE](#)



Ronald Davis

Stanford University

569 PUBLICATIONS 93,170 CITATIONS

[SEE PROFILE](#)



Miloslav Karhanek

Stanford University

21 PUBLICATIONS 592 CITATIONS

[SEE PROFILE](#)

Published in final edited form as:

Nano Lett. 2006 November ; 6(11): 2486–2492. doi:10.1021/nl061681k.

Current Rectification with Poly-L-Lysine-Coated Quartz Nanopipettes

Senkei Umehara^{†,‡}, Nader Pourmand[†], Chris D. Webb[§], Ronald W. Davis[†], Kenji Yasuda^{†,‡}, and Miloslav Karhanek^{*,†}

[†]Stanford Genome Technology Center, Department of Biochemistry, Stanford University, 855 California Avenue, Palo Alto, California 94304

[‡]Department of Life Sciences, Graduate School of Arts and Sciences, The University of Tokyo, 3-8-1 Komaba, Meguro, Tokyo 153-8902 Japan

[§]Stanford University School of Medicine, Stanford University, 855 California Avenue, Palo Alto, California 94304

Abstract

Ion current rectification with quartz nanopipette electrodes was investigated through the control of the surface charge. The presence and absence of a positively charged poly-L-lysine (PLL) coating resulted in the rectified current with opposite polarity. The results agreed with the theories developed for current-rectifying conical nanopores, suggesting the similar underlying mechanism among asymmetric nanostructure in general. This surface condition dependence can be used as the fundamental principle of multi-purpose real-time *in vivo* biosensors.

Nanomaterials are being widely exploited by recent technologies because of their extraordinary properties. Although the development of fabrication processes for particular nanostructures poses great challenges by itself, the practical use of these nanomaterials is also of great interest for biology and medicine.¹ Because of their structural diversity, these materials are often categorized and referred to as nanoparticles,² nanowires,³ nanotubes,⁴ nanopores,⁵ or nanopatterned surfaces.⁶ Nanopipettes are among these; a nanopipette is defined as a pipette with a very fine tip that has a nanoscale opening. Nanolithography is one of the typical applications of nanopipettes as a delivery tool of a tiny amount of chemicals.^{7,8}

Nanopipettes are versatile enough to be used as a tool for sensitive detection in biomedical applications. Optical detection of fluorescently labeled macromolecules such as DNA or proteins with nanopipettes has been reported.^{9,10} Fully electrical detection has also been shown with similarly sized nanoparticles, whose flow through the nanopipette opening creates temporal current blockades.¹¹ The ultimate goal of these efforts, the label-free real-time electrical detection of single molecules, could be achieved eventually by a deeper understanding of the fundamental characteristics of nanopipette electrodes under an external electric field. It not only helps to unveil the dynamics of biological systems but can also have a remarkable impact on drug screening and pathogen detection.

© 2006 American Chemical Society

*Corresponding author. karhanek@stanford.edu. Tel: +1 650 812 1960. Fax: +1 650 812 1975.

Supporting Information Available: Experimental details and procedures regarding nanopipette fabrication, nanopipette coating, electrical measurement, data analysis, and estimation of the effective length as a sensing zone. This material is available free of charge via the Internet at <http://pubs.acs.org>.

Interestingly, although a general understanding of nanopipette electrodes can be based on the understanding of microelectrodes, the unique nanoscale geometry often causes characteristic behavior that requires further focused studies. For example, related studies have examined the physicochemical properties of nanopipettes under varying conditions such as electrolyte concentrations and pH,¹² or polyethylene glycol polymer coatings.¹³ Similarly shaped gold-plated conical nanopores have been studied in a more detailed manner, involving observations of the role of surface charge in the ionic current.¹⁴

Our target here is the effect of cationic polymer coating on a glass nanopipette surface, providing the basis for functionalized nanopipettes that will be used as sensitive biosensors. By understanding how ions flow through the nanometer-sized opening, how these ions interact with the surface inside and outside the tip, and what happens if the surface is modified by the cationic polymer coating, we can obtain practical insight to further functionalize these coated nanopipettes for specific applications. A technical challenge, however, is successful and uniform decoration of the surface of nanopipettes. For example, controlled silanization is said to be extremely difficult when the nanopipette diameter becomes smaller than 200 nm.¹⁵ We overcame this challenge using a hydrophilic, positively charged poly-L-lysine (PLL) polymer as a coating reagent. A stabilized PLL layer created on a nanopipette tip surface is fully functional to other amine-reactive reagents widely available.

Here we compare the fundamental characteristics of the current response between noncoated and PLL-coated nanopipette electrodes to an applied voltage and show that the current signal induced by an identical voltage input was dramatically affected by PLL coating. Noncoated quartz nanopipettes responded to an alternating sine wave voltage input by exhibiting an asymmetric output current, an effect already recognized as current rectification.¹² PLL-coated nanopipettes also rectified the current; however, compared with the noncoated ones, the current was amplified and rectified in an opposite direction. In both cases, current was rectified when the applied voltage amplitude was higher than 10^{-1} V and the frequency was lower than 10^1 Hz, but the exact threshold values likely depend on the surface charge and specific nanopipette geometry. The contribution of surface charge was further confirmed by the measurement under different pH values. The results can be explained in the same way as those obtained by current-rectifying conical nanopores, although nanopipette-specific parameters should be taken into account for quantitative modeling. These current-rectifying nanopipette electrodes have a wide range of potential applications, including their biomedical use as multipurpose real-time *in vivo* biosensors.

Preparation of Nanopipette Electrodes

Experiments were performed with nanopipettes created as reported previously.^{11,16} Figure 1 is a cryo-SEM image of a noncoated, solution-filled nanopipette tip, showing the opening diameter of ~55 nm in this particular case. PLL coating was achieved through a simple wetting with PLL aqueous solution, followed by a baking process for stabilization. The noncoated and PLL-coated nanopipettes were then implemented as electrodes for standard voltage clamp measurements, as shown in Figure 2.¹⁶ Potassium chloride (KCl) was used as the electrolyte. The KCl concentration was set to 25 mM for both the filling and bath solutions, and this ionic strength was maintained throughout the study.

Current Response of Noncoated and PLL-Coated Nanopipettes

To compare the current response of noncoated and PLL-coated nanopipettes, a 1-Hz alternating sine wave voltage with ± 1 V peak-to-peak amplitudes (Figure 3a) was applied to the working electrode inside the nanopipette under test. With noncoated nanopipettes, the current was suppressed during positive half-cycles (Figure 3b). This decrease in amplitude was consistently observed in tens of noncoated nanopipettes. With PLL-coated nanopipettes, however, the

current was oppositely biased; that is, current was higher during positive half-cycles (Figure 3c). This tendency was reproduced with eight PLL-coated nanopipettes, while others showed less-pronounced but still high positive current compared with noncoated nanopipettes. The response with nonbaked PLL-coated nanopipettes was less stable than with baked nanopipettes, suggesting that direct electrostatic binding between the PLL and the quartz surface without free water molecules is required to obtain a stabilized response.

Voltage Dependence of the Current Response

Next we checked the difference between noncoated and PLL-coated nanopipettes over a wide range of applied voltages. A sine wave voltage sweep in 100 mV steps was applied to investigate the input voltage dependence of the current response. The results of three examples are plotted on I - V curves for noncoated (Figure 4a) and PLL-coated (Figure 4b) nanopipettes. Variations among three individual nanopipettes were seen for both conditions. Such variations have been recognized to be caused by differences in the nanopipette geometry.¹⁰ In addition, especially when coated with PLL, surface conditions may also contribute to the variability of the response. Future studies involving precise quantitative and statistical analysis of the observed amplitudes will require a normalization procedure.

The ratio of positive current peaks, I_+ , to negative current peaks, I_- , at the same absolute voltage amplitudes seems suitable for quantifying the extent of rectification.¹⁷ We have introduced its logarithm, $r = \log_2(I_+/I_-)$, to equally deal with positive and negative rectification. Figure 4c shows r values of nanopipettes from Figure 4a and b. All three noncoated nanopipettes exhibited negative r values similar to each other. PLL-coated nanopipettes, however, demonstrated variable r values from zero to positive. This variability apparently derives from the variation of surface coverage of PLL on the nanopipette surface, which results in different net charge density. The data also shows that rectification was pronounced at higher applied voltages in both cases.

Frequency Dependence of the Current Response

The measurements above were all done at 1 Hz. To determine the frequency dependence of the current response, a ± 1 V sine wave voltage between 1 Hz and 1 kHz was applied. For both noncoated and PLL-coated nanopipettes, the response falls into two categories depending on the voltage frequency (Figure 5). At lower voltage frequencies (10^0 – 10^1 Hz), the current amplitude was asymmetric, that is, the current was rectified. Noncoated and PLL-coated nanopipettes rectified the current oppositely. At higher voltage frequencies (10^2 – 10^3 Hz), however, the output current amplitude was symmetric, that is, the current was no longer rectified. The same current amplitude was observed with noncoated and PLL-coated nanopipettes, and the amplitude itself correlated with the frequency in a proportional manner.

Contribution of Surface Charge to the Observed Current Rectification

The results above allow us to characterize noncoated and PLL-coated nanopipettes as negative and positive current rectifiers. It is considered to be caused by the inverted surface charge of the PLL coating. The surface of quartz nanopipettes is negatively charged because of the partial dissociation of the surface silanol groups in pH-neutral solution,¹⁸ whereas the PLL layer makes this surface neutralized and further positively charged because of the protonated primary amine groups of the lysine residues. The contribution of surface charge can be experimentally confirmed by changing the solution pH. The KCl solution without pH adjustment was slightly acidic (pH = 5.0) in our condition. This solution pH was adjusted by the partial replacement of KCl with either HCl (giving acidic conditions that affect negative charges on the noncoated surface; Figure 6a) or KOH (giving basic conditions that affect positive charges on the PLL-coated surface; Figure 6b), and verified every time with commercially available test strips.

Negative surface charge of noncoated nanopipettes should be neutralized at pH values as low as 2.0.¹⁹ When pH 2.0 KCl/HCl was used as both filling and bath solution, the r values of a noncoated nanopipette approached zero (Figure 6a), which means a symmetric current response. This indicates that the negative rectification is indeed due to the negative charge on the quartz surface, as claimed previously.¹⁹ However, the replacement of only bath solution with lower pH KCl/HCl did not achieve fully symmetric current, possibly because of the imbalance of inner and outer H^+ concentrations that cannot be neglected at low pH conditions.

Similarly, increasing pH should affect PLL-coated nanopipettes. Although the state of coated PLL is hard to speculate, pH 9–11 would be a good estimate for neutralization. Therefore, pH 12.0 KCl/KOH was tried for complete compensation of positive charges deriving from PLL. Interestingly, significant negative rectification was observed when a PLL nanopipette was simply dipped into pH 12.0 bath solution (Figure 6b). This negative rectification was much more prominent than that in the case of a noncoated nanopipette in the same pH conditions.

Explanation for the Observed Current Rectification

Our results showed a current rectification effect with quartz nanopipettes, and its inversion upon PLL coating. The observed current rectification effect is consistent with, and supported by, preceding studies of ionic flow through nanopipettes¹² or other hollow structures.^{14,17,20–23} In addition, the inversion of rectification polarity has been confirmed in other nanoporous systems, including chemical modifications of gold-plated conical nanopores with amino-terminated thiols¹⁴ and charged macromolecular chains (DNA and polylysine),¹⁷ as well as silanization of silica nanotubes.²¹ In these papers the modifications rendered the surface charge, resulting in the rectified current with opposite polarity. Despite differences in experimental details such as pore size, material, applied voltage, or ion concentrations, our results with quartz nanopipettes are generally in good agreement with these reports.

The similarity of experimentally observed results in similarly shaped nanostructures suggests that the mechanism underlying the observed phenomena is similar. Therefore, it is attractive to evaluate our own results in the existing context by applying well-established theories on nanofluidic ion transport phenomena. To begin with, we will briefly summarize the related notions proposed so far by the theoretical effort.^{10,12,14,20–21,24–29} (1) The electric potential profile inside the pore governs the transport properties of the pore. (2) The electric potential can be largely influenced by the surface charge, and by the accompanying electrical double layer (EDL). (3) The presence of excess fixed charges can create the imbalance of the numbers of cations and anions in the lumen, resulting in the intrinsic permselectivity of the pore. (4) When an external voltage is applied, the electric potential profile is affected so that it induces the spatiotemporal change of ionic concentration profile, which explains the resulting current-voltage relationship. (5) In the current rectification effect, asymmetry in the electric potential plays a significant role. These notions should be valid in any systems with similar nanostructures as long as the assumptions of the model are satisfied.

As a working model to explain our results, we chose a model proposed by Cervera et al.,²⁴ originally intended for the explanation of current-rectifying conical nanopores. This model was also included in the recent review regarding the rectification in nanopores.³⁰ The model with its assumptions and conditions seems to be best suited for our nanopipette system, especially because it covers a pore dimension larger than the Debye length. The nanopipette radius (~25 nm) and KCl concentration used (25 mM) are within the assumptive range, and the relatively large opening radius should allow the use of continuum models. The only parameter in the model, the surface charge density of -0.16 C/m^2 , is also comparable to ca. -10^{-1} C/m^2 for fused silica.²⁵ Moreover, the presence of a long shank should not matter because the dominant part of the total resistance focuses at the pipette tip region (within a few micrometers of the

tip)¹⁶ where the shape is similar to that of the conical nanopore. Indeed, this geometric similarity has already been reflected in the electric field modeling of nanopipettes¹⁰ and nanopores,²⁶ both independently showing a drastic, highly asymmetric change (i.e., a steep electric potential drop) at the proximity of the tip just inside the pore.

On the basis of these understandings, our results can now be linked to the Cervera model. Note that we intend to show the validity through the qualitative discussion in this Letter. First, the observed current rectification effect could be explained in the same way; that is, by the dynamic change of cation and anion concentrations inside the nanopipette. The enrichment or depletion of particular ions corresponds to the higher or lower current amplitudes, respectively. The consistency was further confirmed by the observation of the concentration dependence of rectification. The rectification effect appeared at or below 100 mM but not at 1 M,¹⁶ giving quantitative agreement with the prediction of the model; it predicts the selectivity of the pore to cations at 0.1 M but not at 1 M when the pore radius equals to 22 nm (Figure 5b in ref 24). Therefore, the different concentrations and pore selectivity can be considered to underlie the current-rectifying nanopipettes.

Second, one can see that current rectification diminishes at high frequencies (Figure 5). Such high frequencies prevent the tip region from reaching its steady state as is assumed in the model; that is, the change of external voltage is too quick to achieve the formation of steady concentration profile at the tip that could represent a low or high electrical conductivity state. The inverse of the threshold frequencies around 10^1 – 10^2 Hz may reflect the time required for full ionic translocation.²⁰

Third, PLL coating inverted the direction of current rectification (Figure 4), and this was reinverted by the high pH condition (Figure 6). This can be explained by the change of the polarity of the surface charge. PLL makes the nanopipette surface positively charged at low and neutral pH, changing the dominant ionic species at the narrow tip region from cations to anions. The high pH condition compensates for the positive charges of PLL, resulting in the recovery of cation-selective pore. Inverting the sign of the surface charge density in the model essentially leads to the exchange of concentration profiles between cations and anions, resulting in the current rectification with opposite polarity.

And last, with PLL-coated nanopipettes, we observed comparable or even more amplified current (Figure 4), and higher sensitivity to external pH change than with noncoated nanopipettes (Figure 6). Again, the surface charge density should be the key. The amplified current can be linked to the higher surface charge density that overcomes the effect of a physically narrowed path by the coated polymers. Such high charge density at the tip could result from the long, hydrophilic PLL chains. It is possible that these chains cause the sensitivity to pH change. Similar speculation has been proposed in the context of nanopores²² in which dangling PLL strands may be present and act as an open–close switch.¹⁷

Although it is possible to compare the qualitative features of the experiment with models, quantitative comparisons are more difficult for several reasons. A major reason is correctly determining the critical parameter, the surface charge density of the Cervera model. The factors that go into determining this parameter are the surface coverage of the PLL layer, electrokinetic processes such as the protonation and deprotonation of hydroxyl and amino groups²¹ under various conditions, and the estimation of the change in zeta potential (and the Debye length) due to the strong external electric field at the tip region. In addition to the surface charge density, building an optimized numerical model may require other nanopipette-specific parameters. The parameters of such a model should reflect differences in nanoscale geometry, material properties, and nanofluidic dynamics. Special attention should be paid to any factors that could differentiate the properties in nanospace from those in bulk. Despite these difficulties,

overcoming these challenges will lead to a design for a nanopipette-based device that controls the ionic flow: an analogue of semiconductor devices.^{23,31}

Future Applications

Understanding the nanopipette properties is an essential step in developing nanopipette biosensors, whose sensing zone is focused at the tip proximity.¹⁶ One direct application of this study could be the use of nanopipettes as pH nanosensors, which would take advantage of their pH dependence of electrical signals. By exploring the sensitivity to the changes of environmental pH, one might be able ultimately to establish a nanopipette-based real-time *in vivo* pH sensor similar to the ion-sensitive microelectrodes,³² which does not require the introduction of optical indicators³³ that could perturb the target cells. The ultrathin tip structure of a nanopipette is particularly suitable for the direct measurements inside single living cells. Targeting specific cellular compartments and intracellular organelles could unveil additional correlations between intracellular pH and cellular functions at a single cell level.

Observing the effect of PLL coating provides insight into additional modification of the nanopipette surface for other purposes. It may also be possible to monitor the functionalization by an amine-reactive reagent because it will affect the surface charge derived from PLL. Even biomolecule detection itself could be possible if the target molecules significantly affect surface conditions. This surface-condition-based detection can be used complementary to or together with current-blockade-based detection, which was already reported for nanoparticles passing through the nanopipette tip.¹¹ That could open up new possibilities to sensitive detection of a wide variety of biomolecules in real time. Metabolite detection upon the exposure to drug candidates, either *in vitro* or *in vivo*, is currently within the reach of this technique.

In conclusion, we have shown that positively charged PLL coating has dramatically changed the ionic current response of quartz nanopipette electrodes to an identical applied voltage. An alternating sine wave voltage input resulted in rectified current in both noncoated and PLL-coated nanopipettes, but the current was amplified and rectified in an opposite direction with PLL-coated nanopipettes. The current rectification was observed with an applied voltage amplitude higher than 10^{-1} V and frequencies lower than 10^1 Hz with dependence on the surface charge. The results were consistent enough with preceding studies using nanopipettes and conical nanopores so that the related theoretical approaches were directly applied to show a common underlying mechanism. The concentration-based explanation proposed by the nanopore community qualitatively validated our results, still leaving room for improvements by introducing nanopipette-specific quantitative parameters. The finding will not only deepen the understanding of physicochemical properties of current-rectifying nanostructure but will also be used as a basis for nanopipette-based *in vivo* biosensors.

Supplementary Material

Refer to Web version on PubMed Central for supplementary material.

Acknowledgments

This work was supported by NIH HG003448 and PO1-HG000205. We gratefully acknowledge the invaluable discussions with our colleagues Henrik H. J. Persson and Jonathan S. Daniels. We are thankful to Dr. Hyonchol Kim for his support in obtaining SEM and cryo-SEM images. We thank Dr. Mathew W. Brock for discussing the practical side of nanopipette fabrication. S.U. and K.Y. acknowledge financial support from Japan Science and Technology Agency.

References

1. Rosi NL, Mirkin CA. Chem. Rev 2005;105:1547–1562. [PubMed: 15826019]

2. Zanchet D, Micheel CM, Parak WJ, Gerion D, Alivisatos AP. *Nano Lett* 2001;1:32–35.
3. Patolsky F, Zheng G, Hayden O, Lakadamyali M, Zhuang X, Lieber CM. *Proc. Natl. Acad. Sci. U.S.A* 2004;101:14017–14022. [PubMed: 15365183]
4. Majumder M, Chopra N, Hinds BJ. *J. Am. Chem. Soc* 2005;127:9062–9070. [PubMed: 15969584]
5. Deamer DW, Akeson M. *Trends Biotechnol* 2000;18:147–151. [PubMed: 10740260]
6. Wadu-Mesthrige K, Amro NA, Garno JC, Xu S, Liu G. *Biophys. J* 2001;80:1891–1899. [PubMed: 11259301]
7. Hong MH, Kim KH, Bae J, Jhe W. *Appl. Phys. Lett* 2000;77:2604–2606.
8. Rodolfa KT, Bruckbauer A, Zhou D, Korchev YE, Klenerman D. *Angew. Chem., Int. Ed* 2005;44:6854–6859.
9. Bruckbauer A, Zhou DJ, Ying LM, Abell C, Klenerman D. *Nano Lett* 2004;4:1859–1862.
10. Ying L, White SS, Bruckbauer A, Meadows L, Korchev YE, Klenerman D. *Biophys. J* 2004;86:1018–1027. [PubMed: 14747337]
11. Karhanek M, Kemp JT, Pourmand N, Davis RW, Webb CD. *Nano Lett* 2005;5:403–407. [PubMed: 15794633]
12. Wei C, Bard AJ, Feldberg SW. *Anal. Chem* 1997;69:4627–4633.
13. Park CW, Knemeyer JP, Marme N, Moller M, Spatz J, Wolfrum J, Sauer M. *Chem. Phys* 2004;301:105–110.
14. Siwy Z, Heins E, Harrell CC, Kohli P, Martin CR. *J. Am. Chem. Soc* 2004;126:10850–10851. [PubMed: 15339163]
15. Li F, Chen Y, Sun P, Zhang MQ, Gao Z, Zhan DP, Shao YH. *J. Phys. Chem. B* 2004;108:3295–3302.
16. See the Supporting Information for details.
17. Harrell CC, Kohli P, Siwy Z, Martin CR. *J. Am. Chem. Soc* 2004;126:15646–15647. [PubMed: 15571378]
18. Senn BC, Pigram PJ, Liesegang J. *Surf. Interface Anal* 1999;27:835–839.
19. Parks GA. *Chem. Rev* 1965;65:177–198.
20. Siwy Z, Fulinski A. *Phys. Rev. Lett* 2002;89:198103. [PubMed: 12443155]
21. Fan R, Yue M, Karnik R, Majumdar A, Yang P. *Phys. Rev. Lett* 2005;95:086607. [PubMed: 16196887]
22. Apel PY, Korchev YE, Siwy Z, Spohr R, Yoshida M. *Nucl. Instrum. Methods Phys. Res., Sect. B* 2001;184:337–346.
23. Karnik R, Fan R, Yue M, Li D, Yang P, Majumdar A. *Nano Lett* 2005;5:943–948. [PubMed: 15884899]
24. Cervera J, Schiedt B, Neumann R, Mafé S, Ramírez P. *J. Chem. Phys* 2006;124:104706. [PubMed: 16542096]
25. Stein D, Kruithof M, Dekker C. *Phys. Rev. Lett* 2004;93:035901. [PubMed: 15323836]
26. Lee S, Zhang Y, White HS, Harrell CC, Martin CR. *Anal. Chem* 2004;76:6108–6115. [PubMed: 15481960]
27. Nishizawa M, Menon VP, Martin CR. *Science* 1995;268:700–702. [PubMed: 17832383]
28. Woermann D. *Phys. Chem. Chem. Phys* 2003;5:1853–1858.
29. Kosińska ID. *J. Chem. Phys* 2006;124:244707. [PubMed: 16821996]
30. Siwy Z. *Adv. Funct. Mater* 2006;16:735–746.
31. Daiguji H, Oka Y, Shirono K. *Nano Lett* 2005;5:2274–2280. [PubMed: 16277467]
32. Voipio, J.; Pasternack, M.; Macleod, K. *Microelectrode Techniques: The Plymouth Workshop Handbook*. 2nd ed. Ogden, DC., editor. Vol. Chapter 11. Cambridge, U.K: Company of Biologists; 1994. p. 448
33. Ohmichi T, Kawamoto Y, Wu P, Miyoshi D, Karimata H, Sugimoto N. *Biochemistry* 2005;44:7125–7130. [PubMed: 15882051]

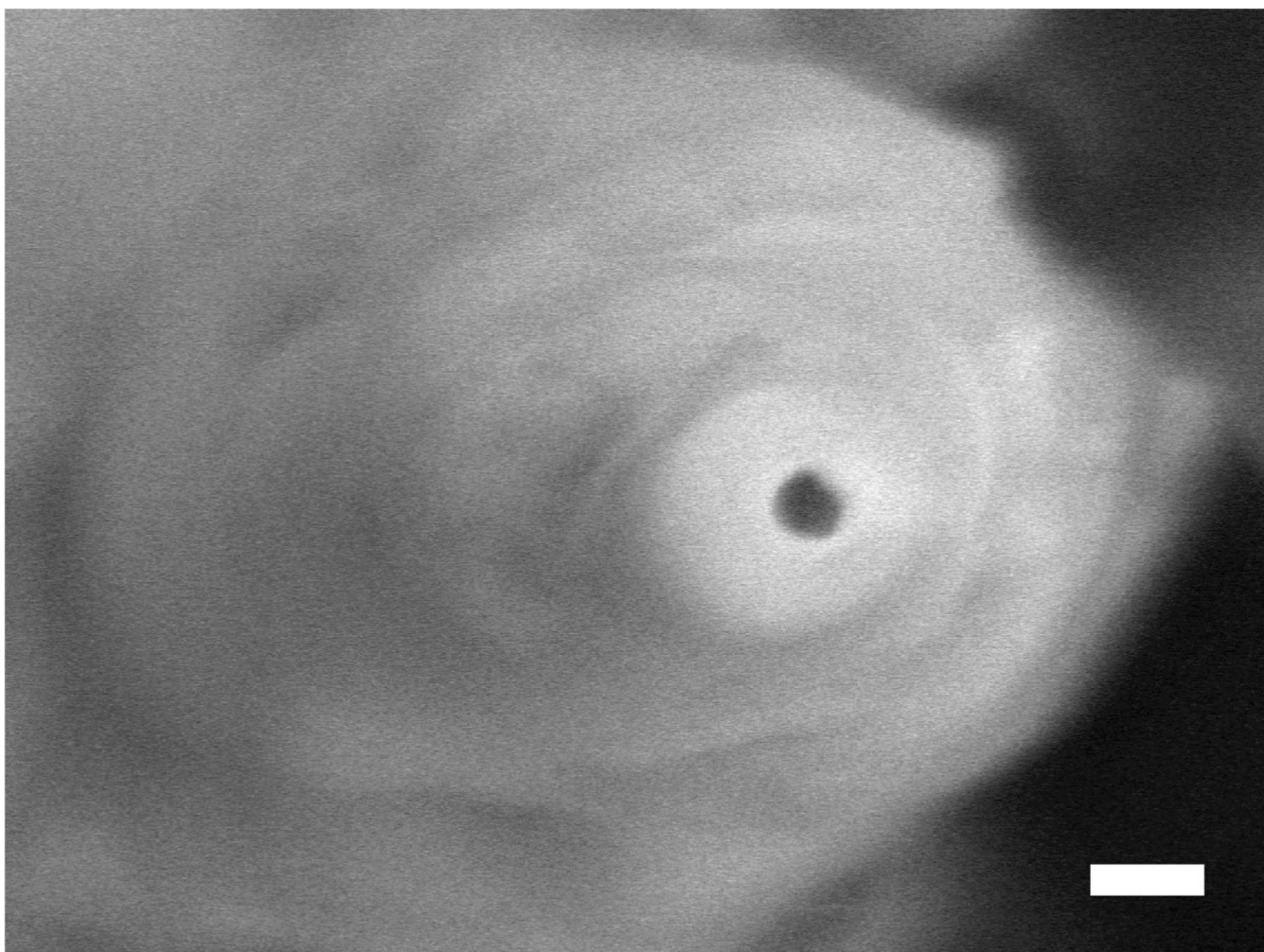


Figure 1. Cryo-SEM image of a typical noncoated, solution-filled nanopipette tip (opening diameter = ~55 nm). Scale bar, 100 nm.

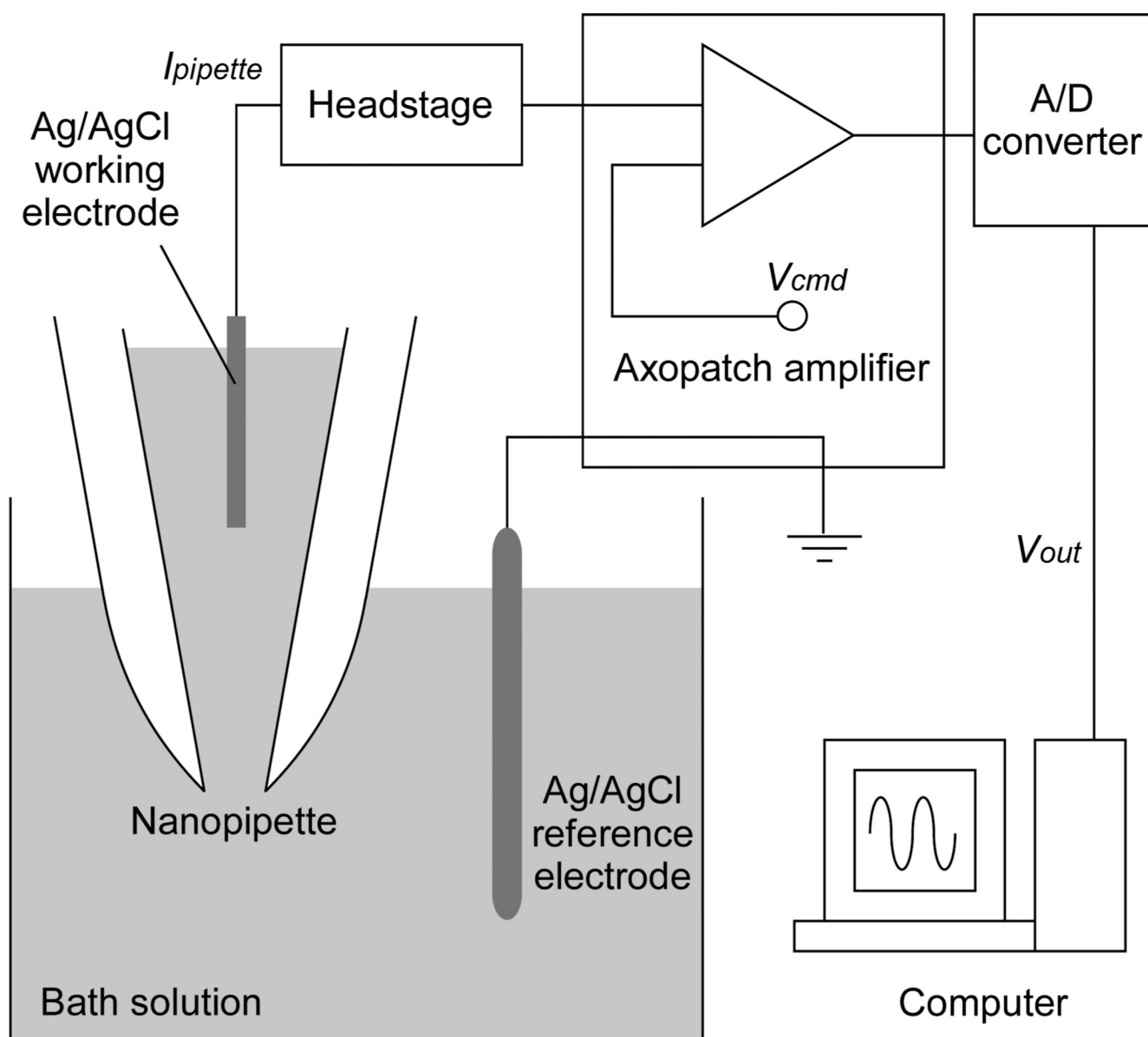


Figure 2. Experimental setup. The electrolyte-filled nanopipette acts as a fine electrode. The current signal (I_{pipette}) was converted to voltage output (V_{out}) and sent to PC through the A/D converter at real time. The amplifier also allows the application of a specific voltage input (V_{cmd}) during measurement.

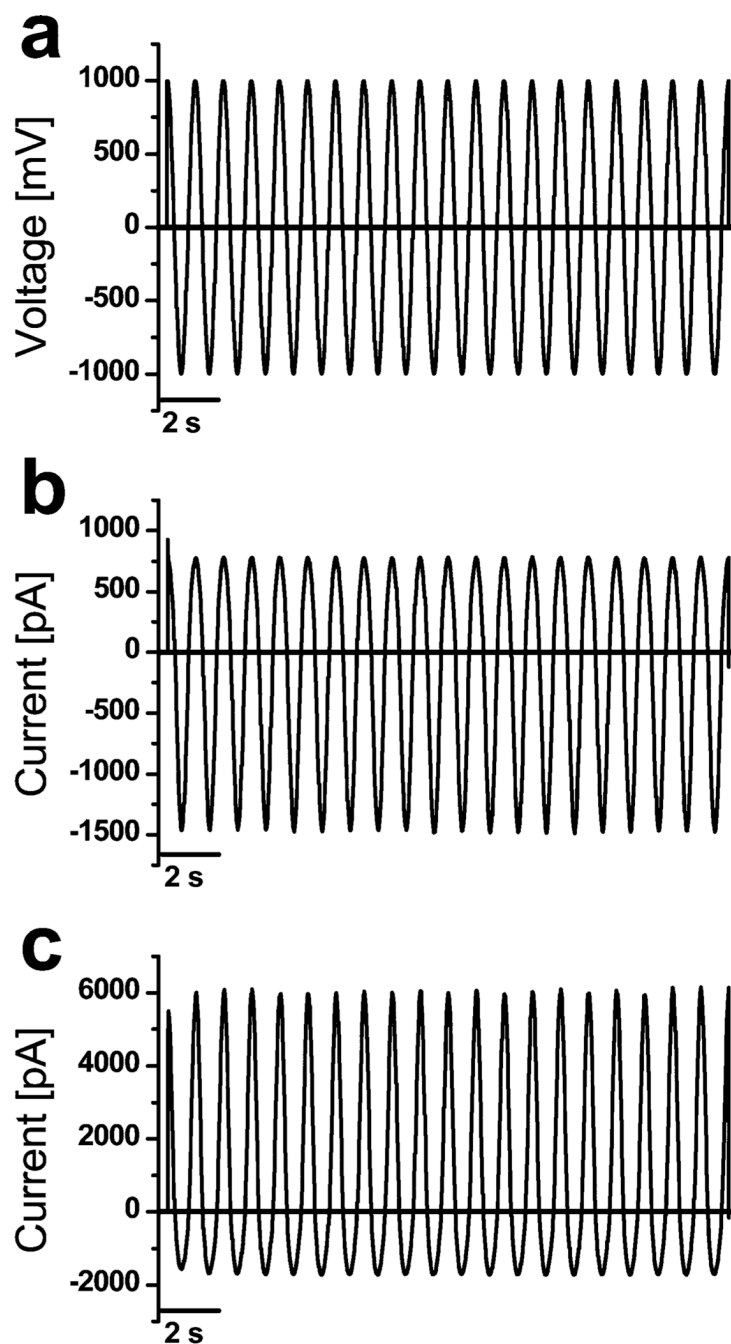


Figure 3.

Examples of the current response of noncoated and PLL-coated nanopipettes. (a) Applied 1 Hz sine wave voltage input. The amplitude and frequency was controlled in the following voltage- and frequency-dependence experiments. (b) Representative current response of a noncoated nanopipette. (c) Representative current response of a PLL-coated nanopipette.

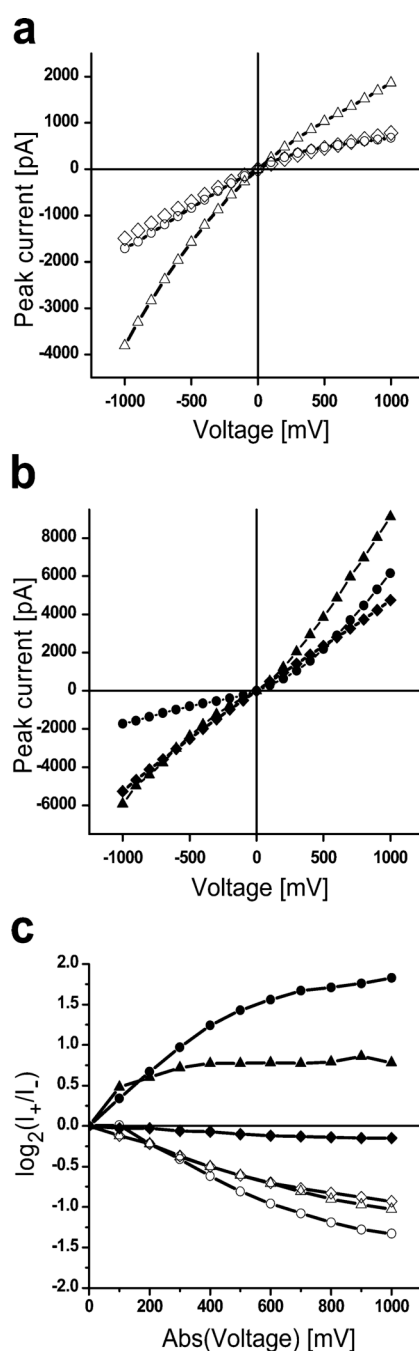
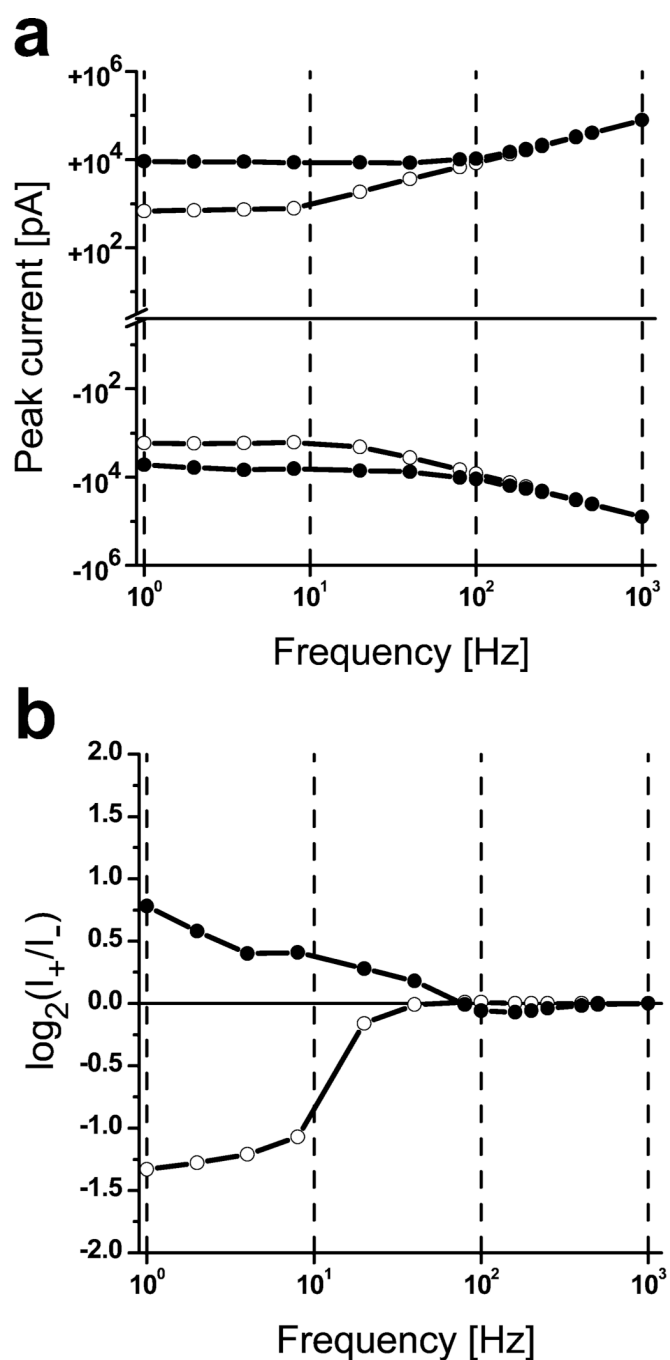
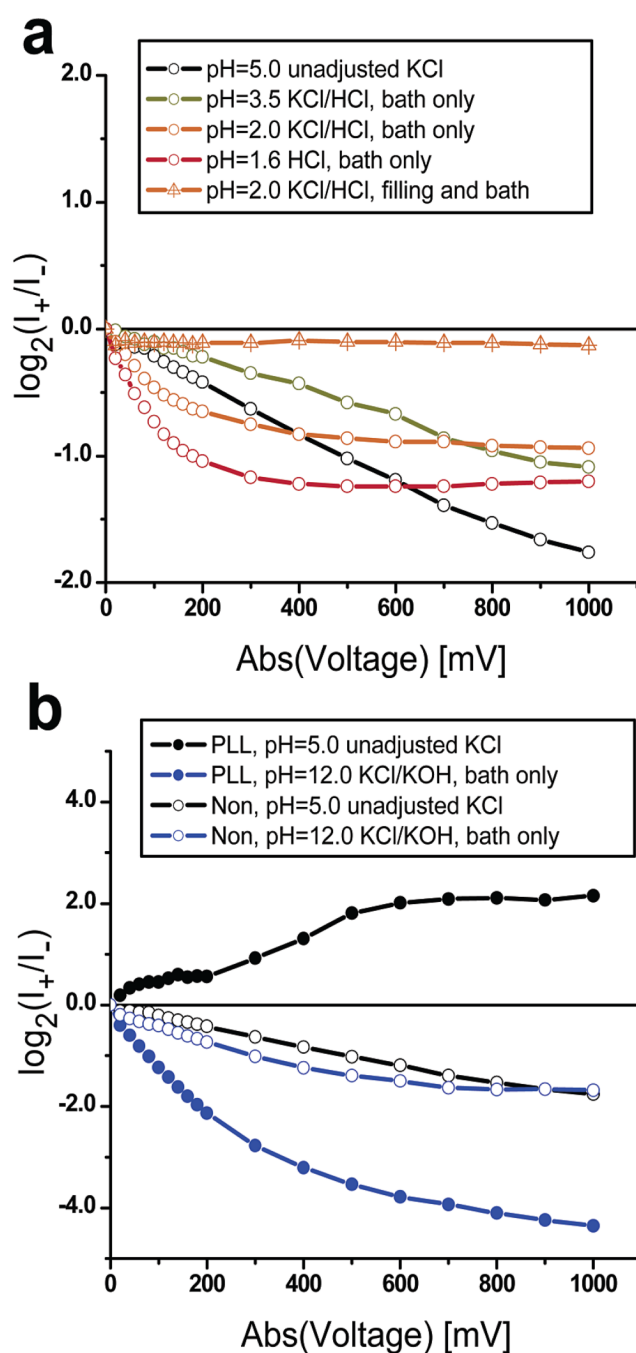


Figure 4.

Input voltage dependence of the current response. Current responses to 1 Hz sine wave voltage sweeps (with 100 mV half-peak amplitude steps from 100 mV up to 1 V) were recorded. Each voltage sweep consists of a sine train of 10 or more periods. The sweep was analyzed to give the positive and negative peak current values to plot current–voltage (I – V) curves. (a) I – V curves for three individual noncoated nanopipettes. (b) I – V curves for three individual PLL-coated nanopipettes. (c) r values (see text for definition of r) for the nanopipettes shown in a and b. Each symbol corresponds to the recorded data obtained with a particular nanopipette.

**Figure 5.**

Input frequency dependence of the current response. A 1 V half-peak sine wave at frequencies between 1 Hz and 1 kHz was applied, and the corresponding positive and negative peak current values were recorded. (a) Current-frequency relationship of a noncoated (open triangles) and a PLL-coated (filled circles) nanopipette. Positive and negative peak current values are plotted symmetrically to clarify the tendency. (b) r values for the nanopipettes shown in a.

**Figure 6.**

pH dependence of the current rectification. (a) Surface charge neutralization of noncoated nanopipettes by acidic conditions. A noncoated nanopipette (open circles) was filled with KCl (without pH adjustment), measured in the same unadjusted KCl bath solution, and then sequentially dipped into other KCl/HCl bath solutions adjusted to different pH. Another noncoated nanopipette (signature triangles) was filled with pH 2.0 KCl/HCl and measured in the same pH 2.0 bath solution. (b) Surface charge inversion of PLL-coated nanopipettes by basic conditions. A PLL-coated nanopipette (filled circles) was filled with unadjusted KCl and measured in the same KCl bath solution, and then moved into a pH 12.0 bath solution. The measurement with a noncoated nanopipette (open circles) followed the same procedure.